Parametric Analysis of the Effects of Friction Coefficient and Site Characteristics on the Sliding Displacement of Sliding Friction Isolation Structures

Xue Wang and Lingyun Peng *

Beijing Key Lab of Earthquake Engineering and Structural Retrofit, Beijing University of Technology, Beijing, China
Email: 940615434@qq.com (L.Y.P.)
*Corresponding author

Manuscript received January 20, 2025; accepted March 7, 2025; published July 24, 2025.

***Abstract*—Current seismic design codes commonly adopt a unified displacement limit to control the sliding response of friction-based isolation structures. However, whether this limit remains adequate under various combinations of earthquake intensity, friction parameters, and site conditions has not been systematically evaluated. This study develops a nonlinear Single-Degree-Of-Freedom (SDOF) finite element model to investigate the influence of friction coefficient, seismic intensity, and site characteristics on the maximum sliding displacement of frictional isolation layers. Three representative site conditions and multiple seismic hazard levels are considered to conduct a series of parametric analyses. The simulated results are compared against the sliding displacement limits specified in current codes to assess their applicability under different parameter combinations. The results indicate that seismic intensity is the dominant factor controlling the magnitude of sliding displacement, while site period has a significant amplification effect, and the friction coefficient exerts a nonlinear regulatory influence on the response. Compared to the code limits, structural responses in hard soil conditions with high friction configurations remain well within allowable ranges, indicating the feasibility of unrestrained isolation design. In contrast, under soft soil, strong ground motions, and low friction coefficients, sliding displacements frequently exceed the prescribed limits, suggesting that appropriate displacement-restricting devices are required. The findings highlight the limitations of uniform displacement thresholds under complex conditions and provide preliminary insights for establishing a more refined, graded approach to displacement limit design.**

***Keywords*—sliding friction isolation, maximum sliding displacement, friction coefficient, seismic intensity, site characteristic period**

I. INTRODUCTION

China is among the countries most severely affected by seismic disasters. Frequent earthquakes have significantly impacted the nation's socioeconomic development [1, 2]. As traditional "hard" seismic resistance technologies encounter limitations, base isolation techniques offer a novel approach. By incorporating isolation layers, these techniques effectively decouple the superstructure from seismic ground motions, thereby reducing the dynamic response of the upper structure. Building upon this concept, sliding friction isolation systems have been developed. These systems introduce a frictional sliding layer between the superstructure and the foundation, allowing horizontal movement during seismic events. This mechanism diminishes the dynamic response of the superstructure. Due to the low horizontal stiffness of the isolation layer, the superstructure can be treated as a rigid body, which simplifies internal force distributions and reduces the complexity of component stresses [3–6]. However, while sliding friction isolation systems effectively mitigate structural responses and are cost-effective and easy to construct, they may experience significant displacements under strong earthquakes. Without appropriate friction parameter settings or detailed design, there is a risk of excessive sliding or structural collisions [7].

Recent studies on sliding friction isolation structures have focused on mechanical modeling, seismic response analysis, and optimization of frictional bearings. For instance, Sun Min *et al.* [8] analyzed the effects of friction coefficients, site conditions, and structural stiffness on instantaneous input energy using rural building models. Other researchers have proposed continuous friction models and novel self-centering bearings to enhance energy dissipation and post-earthquake recovery capabilities [9–11]. Despite these advancements, current research often lacks integration of sliding responses with design code limits and does not adequately address the applicability of limit values under various conditions. Specifically, there is a need for clear evaluation methods and data to assess issues such as displacement limits and collision risks. Some regional design codes have begun to impose restrictions on sliding displacements in isolated structures. For example, the "Technical Specification for Sliding Isolation Buildings in Shaanxi Province" (DBJ61/T 92-2014) recommends controlling sliding limits based on seismic intensity. However, this specification does not consider the combined effects of seismic intensity, site conditions, and friction coefficients. While such simplifications facilitate engineering applications, they may not meet the demands of complex scenarios, often necessitating repeated nonlinear time-history analyses and parameter adjustments during actual design processes.

This study systematically analyzes the maximum sliding displacements of sliding friction isolation structures under seismic loading. Nonlinear single-degree-of-freedom models with varying friction coefficients are developed, and multiple representative ground motion records are introduced. The research explores the influence of seismic intensity, site characteristic periods, and friction parameters on sliding responses. Furthermore, the study compares simulation results with code-specified limits to evaluate whether typical scenarios meet design requirements. Based on the findings, recommendations for selecting friction parameters and designing limit devices are proposed. The results aim to provide data support and methodological references for the design and code development of sliding friction isolation structures.

DOI: 10.7763/IJET.2025.V17.1320

II. Materials and Methods

A. Response Mechanism of Sliding Friction Isolation Structures

Sliding friction isolation structures are designed by placing a frictional sliding layer between the superstructure and the foundation. The frictional interface allows relative movement when subjected to seismic excitation, thereby reducing the transmission of seismic energy to the superstructure and mitigating its seismic response.

Sliding friction models can generally be categorized into continuous and discontinuous types [12–15]. In this study, the Coulomb friction model is adopted to describe the sliding behavior.

The frictional force is defined as:

$$F_f = \mu N \operatorname{sgn}(\dot{x}) \tag{1}$$

$$\operatorname{sgn}(\dot{x}) = \begin{cases} 1 & (\dot{x} > 0) \\ -1 & (\dot{x} < 0) \end{cases} \tag{2}$$

where:

- μ is the friction coefficient,
- N is the normal pressure acting on the interface,
- $\operatorname{sgn}(\dot{x})$ is the sign function representing the direction of relative sliding velocity.

The friction force always acts in the opposite direction of sliding motion.

B. Single-Degree-of-Freedom Model and Dynamic Equations

In practical applications, sliding friction isolation structures are mostly used in low-rise buildings where the superstructure is relatively stiff and torsional effects are negligible. Under such conditions, the seismic response of the system can be simplified into a single-degree-of-freedom (SDOF) model. During earthquake excitation, the system frequently switches between two states: a stationary state and a sliding state. The corresponding dynamic equations and transition criteria are introduced as follows [16–18]:

(1) Stationary State

When no relative sliding occurs between the superstructure and the foundation, the isolation layer behaves as a rigid connection. The structure can be modeled as a conventional elastic SDOF system, governed by the following equation:

$$m\ddot{x}(t) + c\dot{x}(t) + kx(t) = -m\ddot{x}_g(t) \tag{3}$$

where:

- m is the mass of the superstructure,
- c is the effective damping coefficient,
- k is the effective stiffness,
- x(t) is the relative displacement of the structure,
- $\ddot{x}_g$ is the ground acceleration in the horizontal direction.

(2) Sliding State

When the inertial force exceeds the threshold of the frictional resistance, relative sliding occurs at the isolation interface. In this case, the friction force dominates the structural response, and the equation of motion becomes:

$$m\ddot{x}(t) + \mu F_f = -m\ddot{x}_g(t) \tag{4}$$

During sliding, the response becomes highly nonlinear, and the displacement is no longer restrained by stiffness. Significant cumulative sliding displacement may occur.

(3) Transition Criteria

The criteria for switching between stationary and sliding states are crucial for accurately modeling the nonlinear behavior of the system. These conditions are expressed as:

- **Initiation of sliding**:

$$|m\ddot{x}(t)| > \mu N \tag{5}$$

- **Termination of sliding**:

$$|m\ddot{x}(t)| \le \mu N \text{ and } \dot{x}(t) = 0 \tag{6}$$

These two conditions define the exact instants when the system transitions between states. Accurate detection of the transition points is essential for determining the magnitude, duration, and accumulation of sliding displacement.

III. Result and Discussion

A. SDOF Sliding Friction Isolation Model and Parameter Configuration

To investigate the influence of the friction coefficient on the maximum sliding displacement of the isolation layer, a nonlinear Single-Degree-Of-Freedom (SDOF) model was developed in SAP2000, incorporating a friction isolation element. The model parameters are set as follows: the mass of the superstructure is $m=3.8\times10^8$ kg, the effective stiffness in the U1 horizontal direction is 1×10^8 kN/m, and the nonlinear stiffness is 6×10^6 kN/m. The friction coefficient is assigned discrete values ranging from 0.04 to 0.14, with an increment of 0.01. This range covers the typical values used in practical engineering, allowing for a systematic analysis of the effect of friction on sliding response behavior.

The following assumptions are adopted to ensure simulation consistency:

1. Only horizontal seismic excitation is considered;
2. The friction coefficient at the sliding interface remains constant throughout the simulation.

B. Ground Motion Input and Site Conditions

According to the site classification criteria defined in the Chinese seismic code GB 50011-2010, three representative seismic scenarios are selected. Due to the lack of direct shear-wave velocity measurements in many projects, the site classification is inferred from the characteristic site period T_g, in line with the code's parametric substitution guidance. Specifically, input motions with T_g values of 0.25 s, 0.45 s, and 0.75 s are selected to represent Class I (hard soil), Class II (medium-stiff soil), and Class IV (soft soil) sites, respectively. For simplicity, these are referred to in this paper as "hard soil", "medium-stiff soil", and "soft soil".

Each site category includes both artificial and natural ground motions. A total of 125 records were selected for the hard and medium-stiff sites (24 artificial, 101 natural), and 106 records for the soft site (24 artificial, 82 natural).

To ensure representativeness, selected records cover a range of earthquake events, station locations, and spectral characteristics. Key parameters such as site location, characteristic period, and source type for representative records are listed in Tables 1–3 (not shown here in full due to space limitations).

Table 1. Seismic wave information for hard soil sites (Tg = 0.25 s) (excerpt)

Number	Seismic Wave Names	Station locations	Period	Source type
1–1	Anza-02_NO_1959	NILAND-FIRE STATION	0.26 s	Natural
1–2	Anza-02_NO_1967	RANCHO MIRAGE-GERALD FORD & BOB HOPE	0.25 s	Natural
1–3	Chalfant Valley-01_NO_546	JG CROWLEY SHEHORN RES	0.27 s	Natural
1–4	Chi-Chi, Taiwan-02_NO_2159	CHY024	0.23 s	Natural
1–5	Chi-Chi, Taiwan-02_NO_2164	CHY029	0.25 s	Natural
1–6	A01-0.02-0.25	-	0.25 s	Artificial

Table 2. Seismic wave information for medium soil site (Tg = 0.45 s) (excerpt)

Number	Seismic Wave Names	Station locations	Period	Source type
2–1	Anza Horse Canyon -01_NO_229	RANCHO DE ANZA	0.46 s	Natural
2–2	Big Bear-01_NO_902	DESERT HOT SPRINGS	0.49 s	Natural
2–3	Big Bear-01_NO_907	HESPERIA-4TH&PALM	0.43 s	Natural
2–4	Big Bear-01_NO_912	LOS ANGELES-CITY TERRACE	0.46 s	Natural
2–5	Big Bear-02_NO_1868	COLTON-3-BLDG HOSPITAL COMPLEX	0.47 s	Natural
2–6	A01-0.02-0.45	-	0.45 s	Artificial

Table 3. Seismic wave information for soft soil sites (Tg = 0.75 s) (excerpt)

Number	Seismic Wave Names	Station locations	Period	Source type
3–1	Big Bear-01_NO_913	LOS ANGELES-TEMPLE&HOPE	0.75 s	Natural
3–2	Big Bear-01_NO_914	LOS ANGELES-UNIV. HOSPITAL GROUNDS	0.79 s	Natural
3–3	Big Bear-01_NO_916	MECCA-CVWD YARD	0.76 s	Natural
3–4	Big Bear-01_NO_918	NEWPORT BEACH-IRVINE AVE.FIRE STATION	0.76 s	Natural
3–5	Big Bear-01_NO_937	TEMECULA-CDF FIRE STATION	0.81 s	Natural
3–6	A01-0.02–0.75	-	0.75 s	Artificial

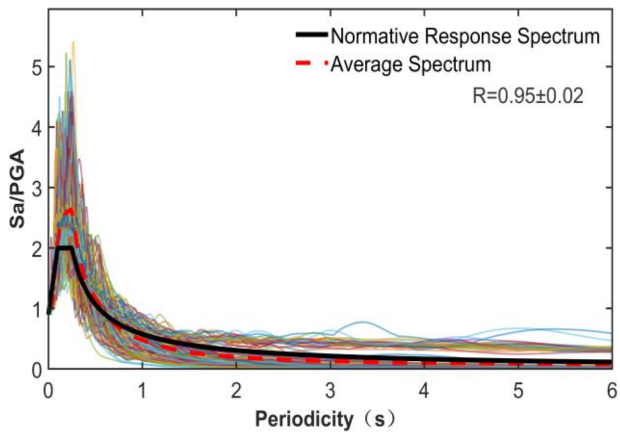

Fig. 1. Comparison curves of response spectra for hard soil sites.

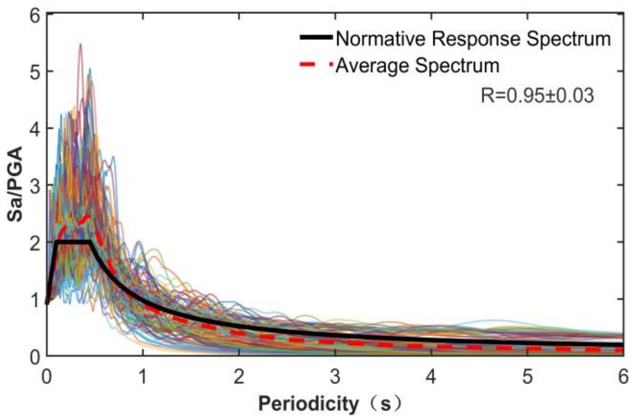

Fig. 2. Comparison curves of response spectra for medium soil sites.

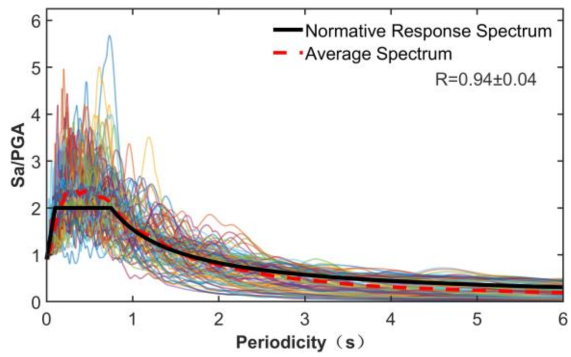

Fig. 3. Comparison curves of response spectra for soft soil sites.

Figs. 1–3 present typical response spectra and mean spectral shapes for the three site conditions. The correlation coefficients of the average spectra for each site type exceed 0.85, and the standard deviation of spectral values is below 0.25g. This confirms that the selected motions are consistent with code requirements in terms of intensity and spectral characteristics.

C. Analysis of Displacement Response

To systematically evaluate the influence of friction coefficient under varying seismic intensities, Peak Ground Accelerations (PGAs) corresponding to 7-, 8-, and 9-degree design levels for both frequent and rare earthquakes are considered, as defined by the seismic code. Figs. 4 and 5 show the trends of maximum sliding displacement versus friction coefficient for different site types and seismic intensities.

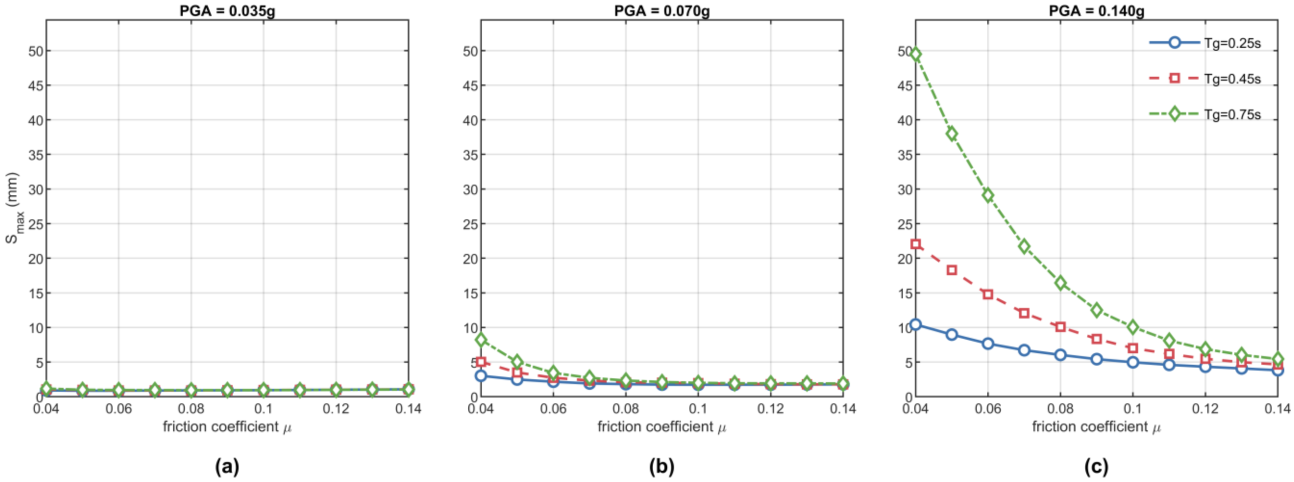

Fig. 4. Maximum displacement versus friction factor for different site characteristics under multiple earthquakes.

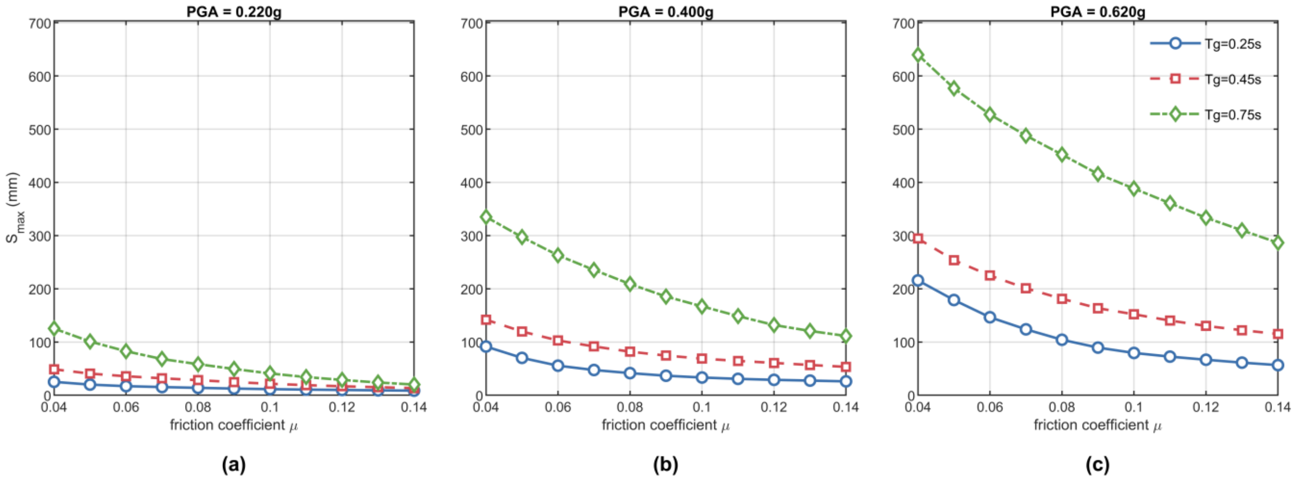

Fig. 5. Maximum displacement versus friction factor for different site characteristics under rare earthquakes.

The results demonstrate that sliding response is jointly influenced by ground motion intensity, site characteristics, and friction coefficient.

1)Dominant role of seismic intensity

Using the simulation data for frequent and rare earthquakes at the 7-, 8-, and 9-degree design levels, the maximum average displacement under each site condition is extracted. For each intensity level, the value represents the maximum among the average displacements across all friction coefficients. The results are shown in Fig. 6.

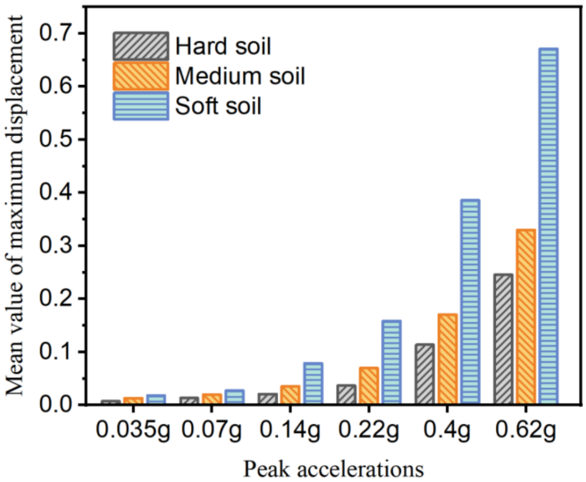

Fig. 6. Mean maximum displacements for site conditions at different seismic intensities.

The results indicate that PGA is the dominant factor controlling the scale of sliding displacement. As seismic intensity increases, displacement response exhibits a stepwise amplification. For instance, in hard soil (with T_g = 0.25 s), the average maximum displacement increases from approximately 2 mm under a 7-degree frequent earthquake (PGA = 0.035g) to 36.7 mm under a 7-degree rare earthquake (PGA = 0.22g), a 19-fold increase. At the 9-degree rare earthquake level (PGA = 0.62g), the maximum displacement reaches 245 mm, more than 122 times the original value. This highlights the nonlinear amplification of sliding under strong seismic events.

This trend aligns with the working mechanism of sliding friction isolation systems. Under frequent earthquakes, most isolators do not trigger sliding, and the overall deformation remains limited. In contrast, under rare earthquakes, the isolators are widely activated, and the structural response intensifies, leading to substantial sliding displacement. Therefore, seismic intensity is the key parameter controlling the maximum sliding displacement. In high-intensity seismic zones, limit or re-centering devices should be designed accordingly to ensure displacement control and structural safety.

2)Amplification effect of site characteristic period

To quantify the influence of site period, friction coefficients are grouped into three ranges: low (0.04–0.07), medium (0.08–0.11), and high (0.12–0.14). For each group, displacements are normalized using the average maximum displacement in hard soil as a baseline (value = 1). Figs. 7 and 8 illustrate the comparative displacement amplification across different site conditions under the same seismic intensity.

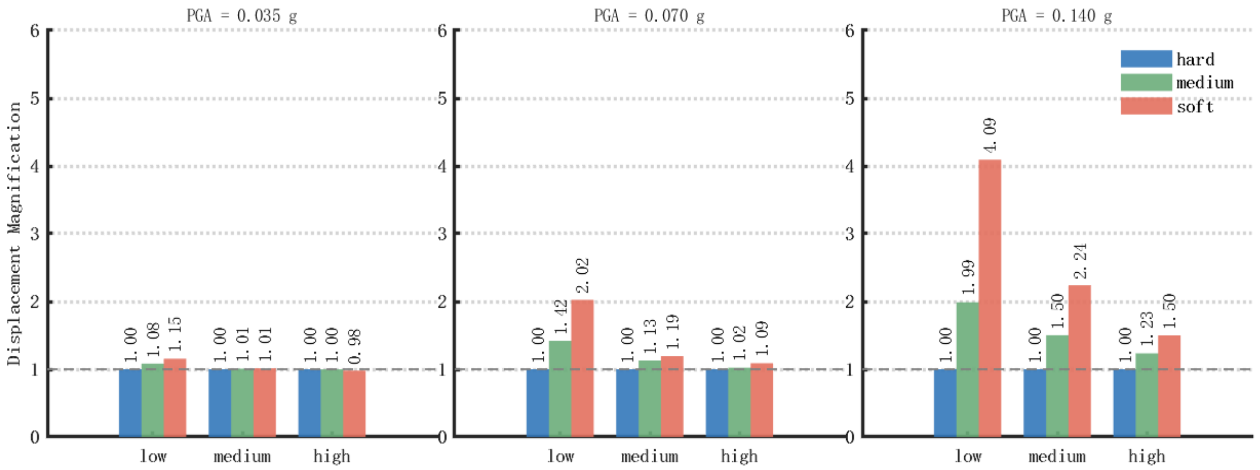

Fig. 7. Comparison of magnification of displacement multiples for multiple earthquake intensities.

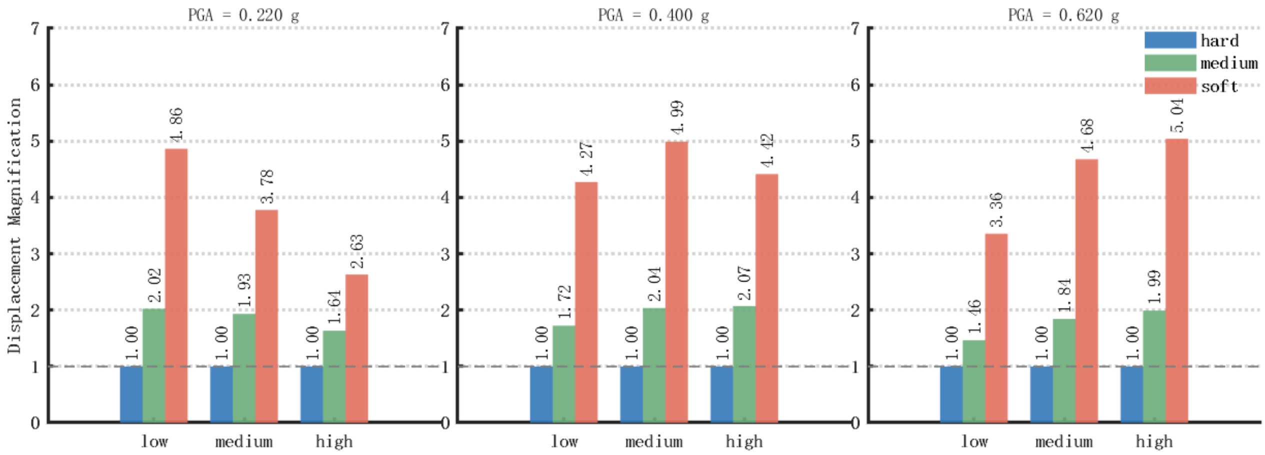

Fig. 8. Comparison of magnification of displacement multiples for multiple earthquake intensities.

The results show that site period has a significant amplifying effect on sliding displacement, which is jointly influenced by seismic intensity and friction coefficient. Under the same conditions, longer site periods lead to stronger sliding responses. For example, in a 9-degree rare earthquake, the average displacement in soft soil is approximately 4.4 times that in hard soil.

Moreover, a comparison between frequent and rare earthquakes reveals distinct behaviors. In frequent earthquakes, low-friction systems are more sensitive to site period, and amplification increases with PGA. In rare earthquakes, high-friction systems become increasingly responsive to site period, even surpassing the amplification of low-friction systems. This is attributed to the lower sliding threshold in low-friction systems, which leads to early saturation, while high-friction systems exhibit delayed but growing sliding potential under prolonged strong shaking.

The amplification effect results from the combined influence of sliding initiation probability and energy accumulation. Soft soils, characterized by long-period, low-frequency seismic content, readily activate sliding, especially in low-friction systems. Their long-duration input and energy concentration near structural resonance frequencies further encourage sustained sliding and displacement accumulation. In contrast, hard and medium-stiff sites typically generate short-period, pulse-like ground motions, which are less effective at sustaining sliding.

Overall, the amplification of sliding response in soft soil conditions is pronounced, particularly under low friction and strong motion. Appropriate selection of friction parameters can effectively control sliding initiation and response levels under different site conditions, which is critical for achieving desired isolation performance.

3)Regulatory role of friction coefficient

There is a notable nonlinear relationship between the friction coefficient and the maximum sliding displacement of the structure. The regulatory effect varies depending on seismic intensity and site condition. To explore this behavior, simulations are conducted under both frequent and rare earthquake conditions for the 8-degree design level, across all three site types. Figs. 9 and 10 illustrate the resulting trends and dispersion characteristics.

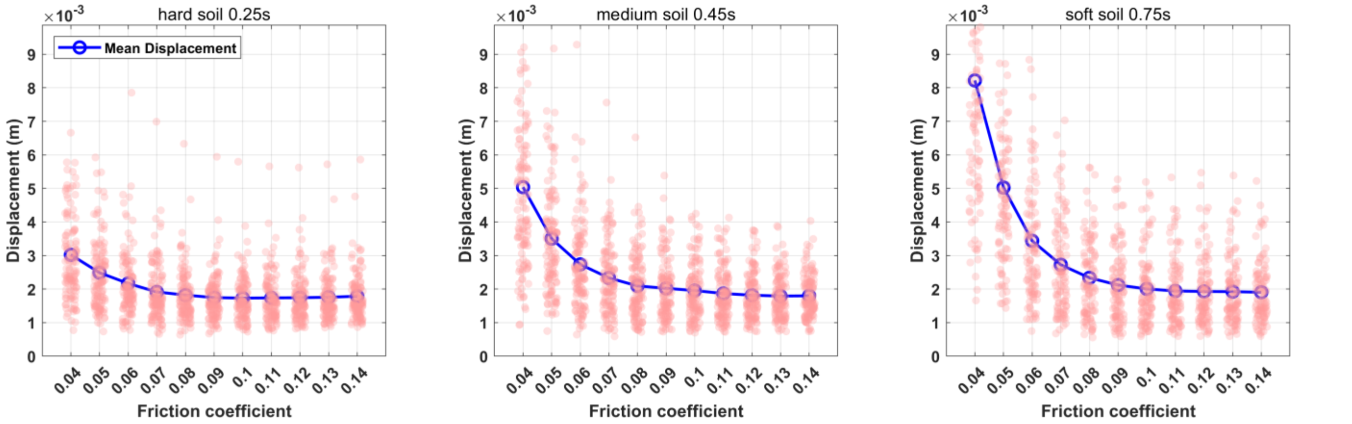

Fig. 9. Curve of maximum slip displacement of isolation layer versus friction coefficient for different sites under 8-degree multi-occurrence earthquake.

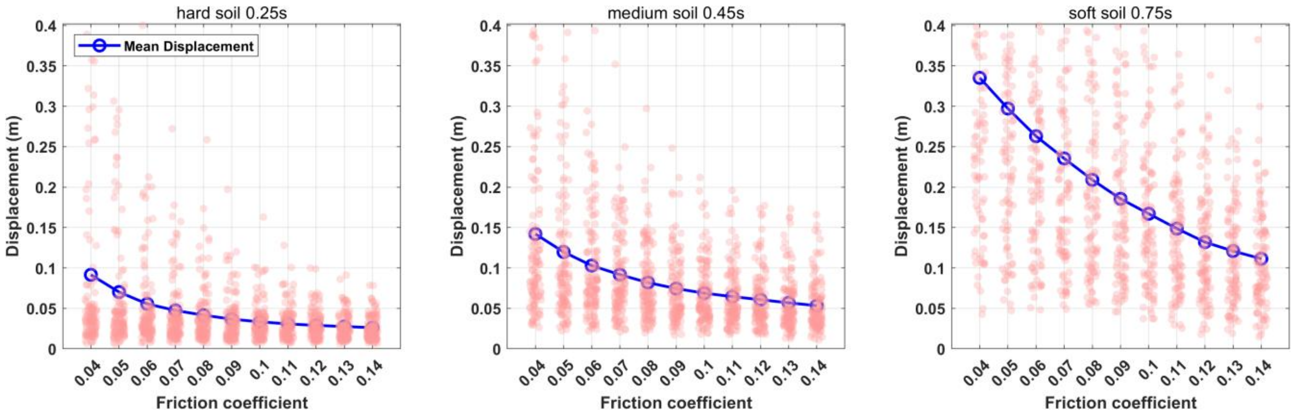

Fig. 10. Maximum slip displacement of isolation layer versus friction coefficient for different sites under 8 degrees rare earthquakes.

The results show that the overall sliding displacement tends to decrease with an increase in the friction coefficient. This trend is especially evident in the low-friction range (μ = 0.04–0.08), where the reduction is more pronounced, indicating a high degree of sensitivity. Under frequent earthquakes, the seismic input is relatively weak, and sliding is not significantly triggered. Consequently, the structural displacement response remains small, and the mean displacement only slightly decreases with increasing friction coefficient. In this case, the regulatory effect of friction is limited.

In contrast, under rare earthquake conditions, the regulatory role of the friction coefficient becomes more apparent, with steeper response curves. Strong seismic input widely activates sliding in isolation bearings, leading to a considerable increase in sliding displacement. While low friction coefficients allow early sliding initiation, the lack of sufficient frictional resistance leads to poor displacement control. As the friction coefficient increases, the sliding threshold rises, restricting the displacement response. However, even at higher friction levels, strong earthquakes can still induce notable sliding, revealing a limitation in the control capacity of friction parameters under extreme conditions.

From the perspective of dispersion, increasing the friction coefficient not only reduces the mean displacement but also narrows the range of response dispersion, particularly in medium-stiff and hard soil conditions. However, as seismic intensity and site period increase, the reduction in dispersion becomes less significant, suggesting that the tuning effect of friction may be limited under long-period or high-intensity scenarios.

In summary, the friction coefficient exhibits a clear nonlinear regulatory effect on sliding displacement under different seismic intensities and site conditions. In frequent earthquakes, the system largely remains in the stationary state, and friction has minimal impact. Under rare earthquakes, sliding responses become dominant, and the role of friction becomes more critical. This effect varies by site type. In soft soil conditions, the response is most sensitive to changes in friction, and control becomes more difficult due to long-duration seismic input and concentrated energy. Therefore, a well-chosen friction coefficient is essential to controlling displacement magnitude and variability, enhancing both the performance and safety of sliding friction isolation systems across various seismic and geotechnical conditions.

D. Comparison of Sliding Displacement and Code Limits

In seismic design, the maximum sliding displacement is a critical parameter for ensuring overall structural safety and determining the size of isolation components. If the displacement exceeds allowable limits, issues such as bearing uplift, damage to restraining elements, or even structural instability may occur. Thus, proper control of sliding displacement and its coordination with limit devices is essential for effective energy dissipation and safety.

Currently, there is no unified national standard for sliding friction isolation structures. Design parameters are often guided by regional or enterprise-specific codes. Nevertheless, most existing codes specify control requirements for the maximum deformation of isolation layers. For example, the

Shaanxi Province Technical Specification for Sliding Isolation Structures (DBJ61/T 92-2014) stipulates in Clause 5.2.2 that the envelope value of maximum sliding displacement S_{max}, calculated from multiple rare earthquake scenarios, should be less than the specified design limit. Additionally, the available sliding space of the bearing should not be less than 1.5 times the larger of S_{max} or the code-specified limit. The design limits are stratified by seismic intensity, as outlined in Table 4 of the specification.

Table 4. Design slip limits for diaphragm layers in Shaanxi Province code

Fortification Intensity	7	8	9
Designed Slip	75 (100)	150 (200)	250

Note: Values in parentheses are for areas where the design base seismic acceleration is 0.15g and 0.30g, respectively.

While this approach offers a baseline for design, it mainly considers seismic intensity and regional zoning, without fully accounting for ground motion characteristics, site period, and friction coefficient effects. As a result, the sliding response may exceed limits in conditions involving soft soil, strong ground motion, or low friction.

1) Comparison between simulation and code limits

To assess the displacement control capacity of sliding friction isolation structures under different scenarios, and their compatibility with the DBJ61/T 92-2014 code, this study compares simulated maximum sliding displacements with code limits across rare earthquake cases.

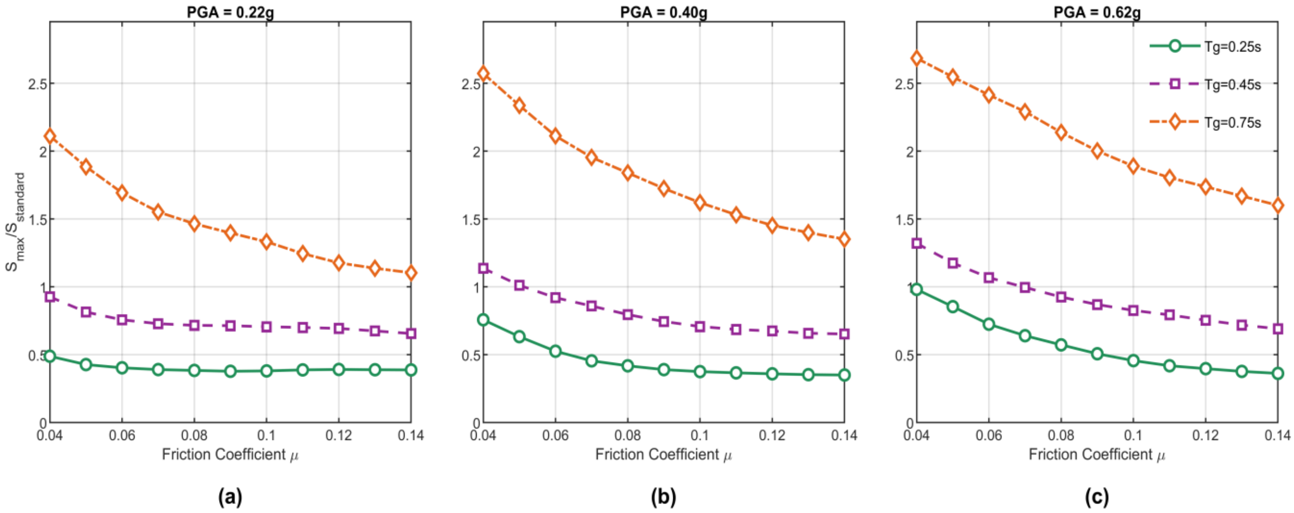

Fig. 11. Ratio of maximum slip displacement to code limit for rare earthquakes.

The results indicate that, in hard soil conditions, the sliding displacement is consistently well below the design limit. In all scenarios, the displacement-to-limit ratio remains less than 1, and even drops below 0.5 in some cases, indicating that unrestricted isolation systems are feasible. In medium-stiff soils, sliding displacement is more sensitive to the friction coefficient. Low-friction cases under strong ground motion approach the code limit, but can still be controlled by tuning the friction parameter. In soft soils, a significant amplification effect is observed. For low friction and high seismic intensity combinations, the displacement-to-limit ratio exceeds 2.5, indicating that sliding exceeds safe levels. In such cases, the use of limit devices is recommended to ensure structural safety.

In summary, unrestricted isolation is suitable for hard soil conditions, offering both safety and cost efficiency. For medium-stiff soils, sliding displacement can be effectively controlled by selecting appropriate friction coefficients, enabling flexible use of limit devices. In soft soil conditions, particularly under strong motion and low friction, limit devices are essential, and sufficient sliding allowance should be reserved to ensure structural stability.

Even under the same design intensity, different site conditions and friction parameters lead to significant differences in sliding response. This suggests that the current code's uniform limit approach may be inadequate for handling complex scenarios. Future revisions should consider site classification, friction characteristics, and seismic intensity to develop a more nuanced, tiered limiting mechanism, thereby improving both applicability and scientific rigor.

IV. Conclusion

This study systematically investigated the seismic response characteristics of sliding friction isolation structures under varying earthquake intensities and site conditions. The results demonstrate that such systems exhibit stage-dependent behavior: no sliding occurs under weak seismic input, while strong earthquakes trigger sliding, allowing the isolation layer to effectively limit force transmission and reduce energy input to the superstructure. The maximum sliding displacement is governed by the coupling effects of seismic intensity, site period, and friction coefficient. Specifically, soft soil sites and low-friction configurations result in significantly amplified responses, while friction exhibits a nonlinear regulatory role that can be optimized to suppress excessive displacement. Comparative analysis with current code-based displacement limits reveals that a uniform threshold is insufficient for diverse geotechnical and seismic conditions. In hard soils, unrestricted systems can ensure safety and cost-effectiveness; in medium-stiff soils, sliding control is achievable through friction tuning; in soft soils, limit devices and adequate sliding allowances are essential. These findings underscore the need for future code revisions to incorporate site classification, frictional properties, and seismic demand into a more refined, performance-based displacement control framework, thereby enhancing the applicability, safety, and resilience of sliding isolation systems in real-world engineering practice.

Conflict of Interest

The authors declare no conflict of interest.

Author Contributions

Wang Xue conducted the simulations, analyzed the results, and drafted the manuscript; Lingyun Peng supervised the research, provided methodological guidance, and reviewed the final version; both authors had approved the final version.

Funding

National Natural Science Foundation of China (Grant No. 52178098).

Acknowledgment

The authors would like to thank Prof. Lingyun Peng for his guidance throughout this research, and Minghui Zhao for providing technical support during the modeling process.

References

[1] Y. Q. Gu, X. M. Wang, "Discussion and prospect of earthquake emergency technology in Shanghai under the background of earthquake disaster mitigation modernization," *Science and Technology & Innovation*, vol. 06, pp. 98–101+105, 2025.

[2] L. L. Xie, Z. Qu, "On the civil engineering disaster and its mitigation," *Journal of Natural Disasters*, vol. 25, no. 01, pp. 1–10, 2016.

[3] Y. H. Zhu and X. L. Lv, "Shaking table tests of model building with sliding isolation system under multi-direction ground motions," *Earthquake Engineering and Engineering Dynamics*, vol. 05, pp. 77–84, 2002.

[4] L. J. Wei, J. S. Liu, and X. H. Cao, "Computational analysis on the seismic response analysis of structures with base friction sliding isolation," *Value Engineering*, vol. 35, no 22, pp. 200–203, 2016.

[5] F. Wu, "Test and numerical analysis of isolation effect of nuclear island in non-bedrock site," Institute of Engineering Mechanics, China Earthquake Administration, 2022.

[6] T. Bibi, A. Ali, A. Naeem *et al*., "To investigate different parameters of economic sliding based seismic isolation system," *Journal of Earthquake Engineering*, vol. 28, no. 3, pp. 659-688, 2024.

[7] X. Huang, Z. X. Hu, D. H. Wang *et al.*, "Study on pounding response and width of isolation joint of isolated structure under extreme rare earthquakes," *Earthquake Engineering and Engineering Dynamics*, vol. 43, no. 05, pp. 100–111, 2023.

[8] M. Sun, G. L. Sun, J. Y. Wang *et al.*, "Parameter sensitivity analysis of the instantaneous earthquake input energy for rural building structures supported on sliding base-isolation systems," *Earthquake Resistant Engineering and Retrofitting*, vol. 43, no. 4, pp. 119–127, 2021.

[9] R. S. Jangid, "Computational numerical models for seismic response of structures isolated by sliding systems," *Structural Control and Health Monitoring*, vol. 12, no. 1, pp. 117-137, 2005.

[10] J. Wang, Z. C. Lai, W. J. Li *et al*., "Experimental study on shear performance of self-resetting rigid sliding isolation bearing," *Construction Technology*, vol. 52, no. 3, pp. 66–71, 2023.

[11] J. T. He, Z. C. Lai, W. J. Li *et al*., "Seismic performance analysis of frame structures in high intensity region based on self-resetting rigid sliding isolation bearing," *Construction Technology*, vol. 52, no. 3, pp. 72–79, 2023.

[12] W. M. Ostachowicz, "A discrete linear beam model to investigate the nonlinear effects of slip friction," *Computers & Structures*, vol. 36, no. 4, pp. 721–728, 1990.

[13] A. S. Mokha, M. C. Constantinou, and A. M. Reinhorn, "Verification of friction model of Teflon bearings under triaxial load," *Journal of Structural Engineering*, vol. 119, no. 1, pp. 240–261, 1993.

[14] N. Mostaghel and T. Davis, "Representations of coulomb friction for dynamic analysis," *Earthquake Engineering & Structural Dynamics*, vol. 26, no. 5, pp. 541–548, 1997.

[15] Z. M. Xiong, M. H. Yu, Y. H. Liu *et al.*, "Seismic excitation calculating on base isolated system with sliding layer," *Chinese Journal of Applied Mechanics*, vol. 4, pp. 139–142, p. 169, 2002.

[16] J. S. Liu, "Test and design method research of friction sliding isolation for frame structure," Xi'an University of Architecture and Technology, 2015.

[17] J. S. Liu, S. L. Wang, Y. Shi *et al.*, "Shaking table test for isolated structures supported on slide-limited innovative separated friction sliding device," *Journal of Xi'an University of Architecture & Technology (Natural Science Edition)*, vol. 47, no. 4, pp. 498–502, 2015.

[18] A. W. Fan, "Study on the sliding displacement of sliding isolation structure," Huazhong University of Science and Technology, 2005.